

4-2016

Diffraction Propagation and Recovery of Modulated (including Chaotic) Electromagnetic Waves through Uniform Atmosphere and Modified von Karman Phase Turbulence

Monish Ranjan Chatterjee
University of Dayton, mchatterjee1@udayton.edu

Fathi H.A. Mohamed
University of Dayton

Follow this and additional works at: https://ecommons.udayton.edu/ece_fac_pub

 Part of the [Computer Engineering Commons](#), [Electrical and Electronics Commons](#), [Electromagnetics and Photonics Commons](#), [Optics Commons](#), [Other Electrical and Computer Engineering Commons](#), and the [Systems and Communications Commons](#)

eCommons Citation

Chatterjee, Monish Ranjan and Mohamed, Fathi H.A., "Diffraction Propagation and Recovery of Modulated (including Chaotic) Electromagnetic Waves through Uniform Atmosphere and Modified von Karman Phase Turbulence" (2016). *Electrical and Computer Engineering Faculty Publications*. 358.
https://ecommons.udayton.edu/ece_fac_pub/358

This Conference Paper is brought to you for free and open access by the Department of Electrical and Computer Engineering at eCommons. It has been accepted for inclusion in Electrical and Computer Engineering Faculty Publications by an authorized administrator of eCommons. For more information, please contact frice1@udayton.edu, mschlangen1@udayton.edu.

Diffraction propagation and recovery of modulated (including chaotic) electromagnetic waves through uniform atmosphere and modified von Karman phase turbulence

Monish R. Chatterjee^{1,*} and Fathi H. A. Mohamed¹

¹Department of Electrical & Computer Engineering
University of Dayton, Dayton, Ohio 45469

*Corresponding author

ABSTRACT

In a parallel approach to recently-used transfer function formalism, a study involving diffraction of modulated electromagnetic (EM) waves through uniform and phase-turbulent atmospheres is reported in this paper. Specifically, the input wave is treated as a modulated optical carrier, represented by use of a sinusoidal phasor with a slowly time-varying envelope. Using phasors and (spatial) Fourier transforms, the complex phasor wave is transmitted across a uniform or turbulent medium using the Kirchhoff-Fresnel integral and the random phase screen. Some preliminary results are presented comparing non-chaotic and chaotic information transmission through turbulence, outlining possible improvement in performance utilizing the robust features of chaos.

Keywords: Atmospheric turbulence modified von Karman spectrum, random phase screen, AM modulation, transfer function, cross-correlation, cross-power spectral density, chaos.

1. INTRODUCTION

In the past few decades, the impact of atmospheric turbulence on both the amplitude and phase of propagating EM signals have been investigated extensively [1]. The consequence of (random) phase fluctuations of the transmitted signal in distorting the amplitude of the received signal may be established both experimentally and via numerical simulation. Usually, phase turbulence is modeled using one or more random phase screen(s) placed at certain locations between the aperture plane and the observation plane [2,3]. The traditional models for turbulence (including Kolmogorov, Tatarski, von Karman, and modified von Karman) assume homogenous and isotropic [4]. In our recent work, transfer function formalism was applied to examine the propagation of modulated chaos waves through atmospheric turbulence [5]. The turbulence was modeled via a random phase screen placed half way between the aperture and image planes. This random phase screen is created using the modified von Karman turbulence model. The overall propagation problem is analyzed within the framework of a linear system and thereby an equivalent transfer function model is derived from cross- and self- (power) spectral densities using chaos and turbulence simultaneously. Later, as reported in [6], a modulated chaos wave as the input EM field was incorporated where the power spectral density (PSD) of the modulated chaos wave ($S_{Cm}(f)$) was calculated via an auto-correlation function ($R_{Cm}(\tau)$) using the (effectively random) chaos field amplitude. By defining a corresponding turbulence transfer function $H_T(f)$ derived from [5] based on spectral densities, a cross-power spectral density ($S_{TCm}(f)$) and cross-correlation function ($R_{TCm}(\tau)$) between the modulated chaos and turbulence were obtained. Recovery of the actual information from the above cross-correlation poses additional physical and mathematical complexity; the work so far therefore is under further examination. In a parallel approach, which is the subject of this paper, the diffraction of a time-modulated plane EM wave through both a uniform and a phase-turbulent atmosphere is currently under study, and some results from this approach are presented in this paper. Specifically, an input EM wave is treated as a modulated optical carrier represented by use of a sinusoidal phasor with a slowly time-varying envelope (SVEA) due to the (time-dependent, non-sinusoidal) information signal. Using a combination of phasors and spatial Fourier transforms, the resulting complex phasor wave is then transmitted across the propagation path (with or without turbulence) through the dual use of the Kirchhoff-Fresnel integral and the random phase screen. The objective is to ascertain if the presence of turbulence imparts any amplitude and/or phase distortion in the embedded message carried by the EM carrier. In the follow-up work, the transmitted EM wave is assumed to be an encrypted chaotic carrier, for which a similar phasor-Fourier transform approach may be applied to determine the recovery via demodulation of the information encrypted on the chaos as it propagates through the turbulence. Some preliminary

results are presented via comparisons between non-chaotic and chaotic information transmission through atmospheric turbulence, outlining thereby any possible improvement in system performance by utilizing the robust features of chaos. The organization of this paper is as follows. In section 2, propagation through turbulence using cross spectral densities and transfer functions are discussed. A Spectral approach to propagate the (non-chaotic) EM waves through turbulence using SVEA and Fourier transforms is outlined in section 3. Numerical simulations and results for the propagation of *modulated non-chaotic* waves through atmospheric phase turbulence under different conditions are reported in some detail in section 4. In section 5, spectral approach to encrypted chaotic wave propagation through turbulence using SVEA and Fourier transforms is outlined. Numerical simulations and results for the propagation of *modulated chaotic* waves through uniform and turbulent medium are investigated in section 6. Finally, concluding remarks and ideas to further expand the research are presented in section 7.

2. PROPAGATION THROUGH TURBULENCE USING CROSS SPECTRAL DENSITIES AND TRANSFER FUNCTIONS

In this section, we will discuss the overall mathematical approach to analyzing the propagation of EM waves starting from the aperture plane through homogeneous space up to a random phase screen (representing narrow phase turbulence) and thereafter continuing diffractive propagation until arriving at the image plane.

2.1 Split-step approach to EM propagation via diffraction and turbulence

In this subsection, we briefly review the basic concepts behind using the so-called split-step approach to EM wave propagation alternately via spatial diffraction and regions of narrow turbulence. A similar (though not identical) technique, called the split-step beam propagation method (SSBPM) is a numerical technique commonly applied to solve nonlinear partial differential equations such as the nonlinear Schrödinger equation (NLS). The method relies on computing the solution in small steps taking into account the linear and nonlinear (or non-deterministic) steps [7,8]. In applying the split-step approach, we next transmit the scalar output field over an incremental distance Δz and find the diffracted field at this distance by using the familiar Fresnel-Kirchhoff diffraction integral, which will be briefly outlined in the next subsection. In the case of the extended random phase turbulence, where this approach has been recently applied, the field output is then passed through subsequent random phase screens multiple times as needed, and finding the output for each random phase.

2.2 Fresnel-Kirchhoff diffraction integral

A general schematic for aperture diffraction of plane EM waves is shown in Fig.1. Shown in the figure are the object or aperture plane (with coordinates x_0, y_0), the image plane (with coordinates x_i, y_i), and the radial distance r between points in the object and image planes [9]. Starting with the familiar Rayleigh-Sommerfeld and Huygens-Fresnel principles applied to generalized EM wave diffraction through a homogeneous medium, and after applying a series of assumptions including paraxial and binomial approximations and zero obliquity [10], one may write:

$$(x_0, y_0), (x_i, y_i) \ll z_i, \quad \text{and} \quad (1)$$

$$r_{01} \approx z_i \left[1 + \frac{1}{2} \left(\frac{x_i - x_0}{z_i} \right)^2 + \left(\frac{y_i - y_0}{z_i} \right)^2 \right], \quad (2)$$

where r_{01} is the radial distance between object and image plane points, (x_0, y_0) and (x_i, y_i) represent the object and image point coordinates, and z_i is the longitudinal distance.

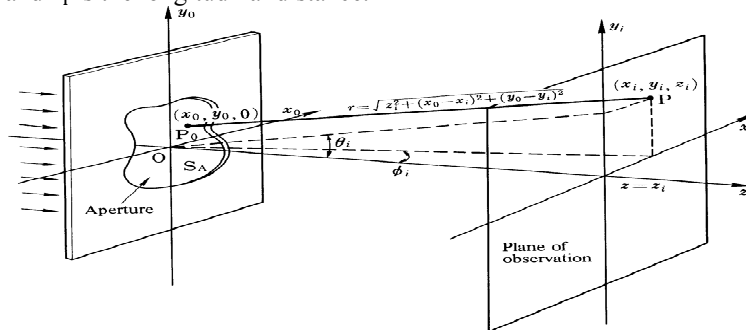


Fig.1. Geometry representation of the aperture and observation planes.

With the above approximations, the above equation is further approximated to the familiar Fraunhofer diffraction formula [11,12]:

$$U(x_i, y_i) = \frac{e^{jkz_i}}{j\lambda z_i} \frac{e^{jkz_i}}{j\lambda z_i} e^{j\frac{k}{2z_i}(x_o^2 + y_o^2)} \iint_{-\infty}^{\infty} U(x_o, y_o) e^{j\frac{2\pi}{\lambda z_i}(x_i x_o + y_i y_o)} dx_o dy_o \quad , \quad (3)$$

which is also expressible as the Fourier transform:

$$U(x_i, y_i) \propto \mathcal{F} \{U(x_o, y_o)\} .$$

where x_i and y_i are related to the spatial frequencies f_{x_i} and f_{y_i} as: $x_i = f_{x_i} \lambda z_i$, $y_i = f_{y_i} \lambda z_i$.

2.3 Cross-correlation and cross-power spectral density functions

For two independent random processes (hereafter referred to by C and T for chaos and turbulence respectively), the cross-correlation $R_{CT}(\tau)$ and cross-power spectral density $S_{CT}(f)$ functions may be given as [13]:

$$R_{CT}(\tau) = E(E_C(t)E_T^*(t + \tau)) \quad (4a)$$

and

$$S_{CT}(f) = \mathcal{F} \{R_{CT}(\tau)\} \quad , \quad (4b)$$

where E denotes expectation operation, E_C and E_T denote the scalar chaos and turbulence field amplitudes, and \mathcal{F} denotes Fourier transform.

The effective transfer function ($H_T(f)$) between the chaos and the turbulence may be found using the following formula [5]:

$$H_T(f) = \frac{S_{CT}(f)}{S_C(f)} \quad , \quad (5)$$

where $S_{CT}(f)$ is the cross-power spectral density defined above, and $S_C(f)$ is the power spectral density of the chaos wave.

Using $H_T(f)$ and the modulated chaos wave spectral density $S_{Cm}(f)$, we can compute the cross-power spectral density ($S_{TCm}(f)$) as follows:

$$S_{TCm}(f) = H_T(f)S_{Cm}(f) \quad . \quad (6)$$

We may then compute the cross-correlation function ($R_{TCm}(\tau)$) between the modulated chaos wave and the turbulence by applying the inverse Fourier transform to $S_{TCm}(f)$:

$$R_{TCm}(\tau) = \mathcal{F}^{-1}\{S_{TCm}(f)\} \quad . \quad (7)$$

In recent work, simulation results (not shown here) have been presented indicating the above cross-correlation functions for chaos waves under simple (AM) modulations upon passage through turbulence [6]. Extracting the transmitted information signal from the above cross-correlation presents additional challenges which are currently under further investigation.

3. SPECTRAL APPROACH TO PROPAGATE THE (NON-CHAOTIC) EM WAVES THROUGH TURBULENCE USING SVEA AND FOURIER TRANSFORMS

In this section, we examine the propagation of (non-chaotic) EM waves through atmospheric turbulence and their characteristics in the image plane. Starting with a profiled beam represented by a time-harmonic carrier:

$$E(x, y, z, t) = E_o(x, y, z) \cos(\omega_o t - kz) \quad , \quad (8)$$

with $\vec{k} = k_z \hat{a}_z$, and

$$E_o(x, y, z) = A \frac{w_o}{w(z)} e^{-r^2/w^2(z)} \quad , \quad (9)$$

where $w^2(z) (= w_o^2 (1 + \frac{z^2}{z_o^2}))$ defines the beam spot size; $r^2 = x^2 + y^2$; ω_o is the carrier frequency; w_o is the beam waist, and z_o is the depth of focus of the (Gaussian) beam [14,15].

By substituting eq. (9) in (8), we get

$$E(x, y, z, t) = A \frac{w_o}{w(z)} e^{-r^2/w^2(z)} \cos(\omega_o t - kz) \quad . \quad (10)$$

The (AM) modulated EM wave may be expressed as:

$$E_{AM}(x, y, z, t) = E_o(x, y, z)[1 + ms(t)] \cos(\omega_o t - kz) \quad , \quad (11)$$

where m is the modulation index and $s(t)$ is the modulating signal (message). The above then represents a directly modulated optical carrier.

By substituting eq. (9) in (11), we get

$$E_{AM}(x, y, z, t) = A \frac{w_0}{w(z)} e^{-r^2/w^2(z)} [1 + ms(t)] \cos(\omega_0 t - kz) . \quad (12)$$

Note that the term $A \frac{w_0}{w(z)} e^{-r^2/w^2(z)} [1 + ms(t)]$ is a time-varying spatial envelope defined by the signal waveform.

As we mentioned above, in our approach we will use the SVEA approximation where the envelope varies slowly compared with the rate of change of the optical carrier (i.e., envelope BW $B \ll \omega_0$). This method involves expressing the optical carrier via phasor representation wherein the envelope (containing the signal waveform) is slowly varying in time. The analysis then proceeds with the application of the diffraction integral acting upon the above complex spatial phasor, and the resulting propagation is tracked numerically to the receiver or “image” plane.

Accordingly, we next propagate the modulated EM wave ($E_{AM}(x, y, z, t)$) converted to the phasor domain (while retaining the SVEA envelope) by applying the Fresnel-Kirchhoff diffraction integral along the propagation path. An inverse phasor transform restores the optical carrier. A photodetector recovers the modulated envelope by retaining the intensity profile (which removes the carrier). For a directly modulated optical carrier, the signal is recovered by using appropriate filtering and scaling. On the other hand, if the optical carrier has an envelope containing an RF modulated carrier (such as a modulated chaos wave), recovery would require additional use of heterodyne AM demodulation followed by filtering. At the receiver, the scalar output is proportional to the photodetector current at the point location (say at $0, 0, z_i$ for on-axis detection) where the photodetector intercepts the input field:

$$I_{PD}(t) \propto |E_{out}(0, 0, z_i)|^2 [1 + ms(t)]^2, \quad (13)$$

where $E_{out}(0, 0, z_i)$ is equivalent to the spatial Fourier transform of $E_o(x_o, y_o) e^{-jk_z z} g(x_o, y_o)$ in the far-field *on-axis* with $E_o(x_o, y_o)$ being the profile of the input wave and $g(x_o, y_o)$ being the aperture function through which the wave is transmitted at the “object” plane.

The message signal may be retrieved from the photocurrent via appropriate electronics. This establishes the fact that under homogeneous propagation, a modulated carrier may be demodulated directly using time-domain strategies without having to consider spatial diffraction and other effects. On the other hand, when the intervening medium is turbulent (in phase or otherwise), there is a likelihood that the random spatial effects would affect the signal riding on the carrier wave; hence, one of the goals of this study is to examine the effects of such atmospheric turbulence on the transmitted signal.

4. NUMERICAL SIMULATIONS, RESULTS AND INTERPRETATIONS

In this section, we will examine the propagation of a modulated (non-chaotic) wave through uniform and turbulent media (weak and strong) with effective frequency f_T ($= 20, 50$ and 100Hz). The modulated signal is sent from the aperture plane to the image plane passed through a random phase screen located mid-way of the propagation path. In this approach, to accommodate the temporal variations of the turbulence, the propagation algorithm is applied one pass at a time; thereafter, the resulting spatial output is calculated in the image plane corresponding to that pass. The process is repeated over pre-selected time intervals (representing the average time scale of the turbulence). In this manner, an average time profile of the output is generated taking into account the multiple passes, representing the random output profile influenced by the von Karman turbulence. The parameters used in this simulation are chosen as: inner scale $\ell_0 = 1\text{mm}$; outer scale $L_0 = 1\text{km}$; phase screen grid size and resolution $500\text{mm} \times 500\text{mm}$ and 513×513 pixels respectively; the propagation distance $L = 5\text{km}$.

4.1 A uniform (non-turbulent) propagation prototype

To test the behavior under turbulence, we first present below results from a simple homogeneous, diffraction-limited propagation of a modulated (optical) EM wave through the use of the Kirchhoff-Fresnel diffraction integral. Accordingly, a Gaussian profile beam (Fig.2(a)) is modulated by a sinc-type pulse (Fig.2(b)), and is received as a diffracted Gaussian (Fig.2(c)) with a circular symmetry (Fig.2(d)) and a broadened profile (Fig.2(e)). Fig.2 (f) shows the final recovered signal after carrying out the necessary demodulation operation using the photodetector output.

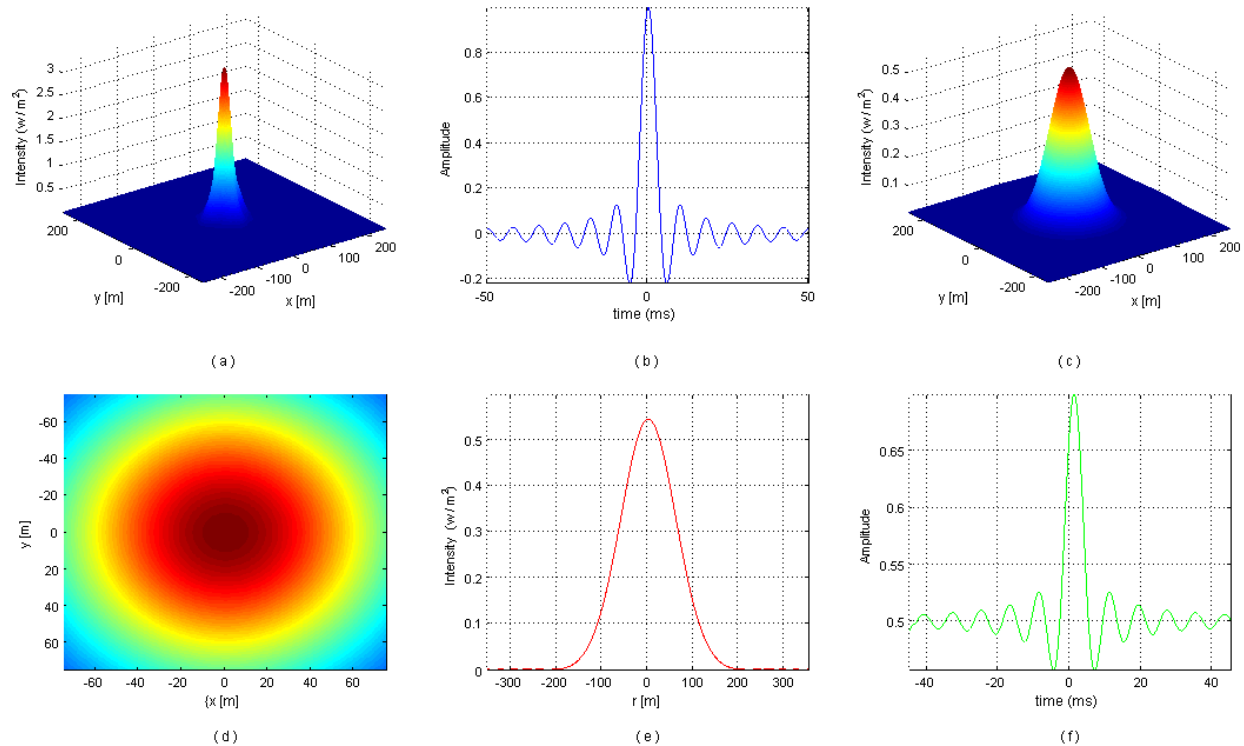


Fig.2. Propagation of EM waves through uniform medium. (a) 3D Gaussian beam input ($w_0 = 30mm$); (b) modulating signal; (c) 3D Gaussian beam output ($w_0 \approx 80mm$); (d) cross-section of the output Gaussian intensity; (e) 2D output Gaussian profile; and (f) recovered signal.

The above figures demonstrate typical spatial transmission and recovery of an EM wave through a homogeneous medium whereby the profiled EM wave (here Gaussian) undergoes diffractive spread; however, the time signal embedded within the optical carrier is simply recovered using standard detection electronics (see Fig.2(b) and (f)). We include this relatively trivial result here simply to enable further understanding as to the consequences on the homogeneous prototype when medium turbulence is incorporated into the problem.

4.2 Propagation through *weak* turbulence

For weak turbulence, we choose Fried parameter $r_0 = 10 \text{ mm}$ with structure parameter $C_n^2 = 1.067 \times 10^{-18} \text{ m}^{-2/3}$. Note that turbulence is typically modeled as a spatial effect; however, in reality it also is subject to random time variations. In our analysis, we incorporate the temporal variation of turbulence by repetitive insertion of the thin phase screen over pre-selected time intervals which thereby defines an equivalent mean (temporal) turbulence frequency.

(a) Propagation through *weak* turbulence with mean frequency $f_T = 20 \text{ Hz}$

In this section, we repeat the procedure described in 4.1 above for a narrow, weakly turbulent medium. To represent the time fluctuations of the medium phase, the narrow phase screen is inserted into the propagation algorithm (at the half-way distance) repeatedly every (1/20) second, thereby generating random results at a mean turbulence frequency of 20 Hz.

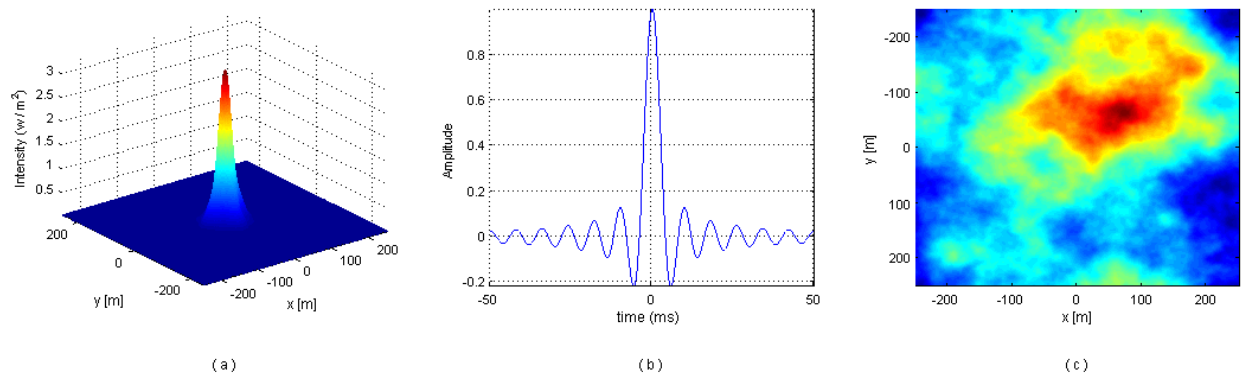


Fig.3. Propagation of EM waves through weak turbulence ($f_T = 20\text{Hz}$). (a) 3D Gaussian beam input ($w_0 = 30\text{mm}$); (b) modulating signal; and (c) random phase screen distribution profile.

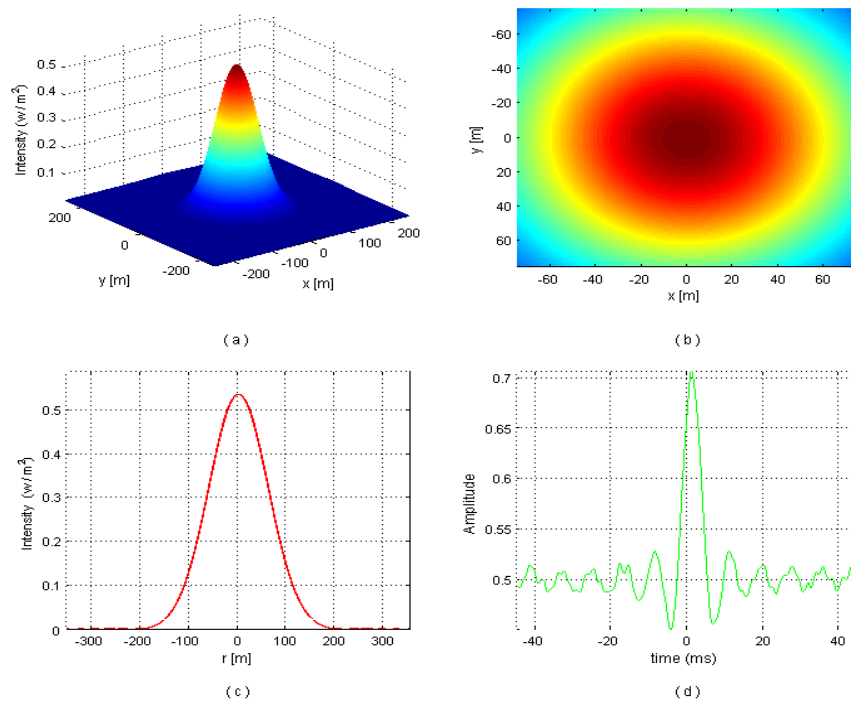


Fig.4. Propagation of EM waves through weak turbulence ($f_T = 20\text{Hz}$). (a) 3D Gaussian beam output ($w_0=80\text{mm}$); (b) cross-section of the output Gaussian intensity; (c) 2D output Gaussian profile; and (d) recovered signal.

The results above show that under weak phase turbulence, the recovered signal upon averaging the repeated time profiles for each pass over the 20 Hz turbulence is beginning to exhibit some distortion (Fig.4 (d)).

b) Propagation through *weak* turbulence with mean frequency $f_T = 50\text{ Hz}$

In this section, we repeat the same procedure for 50 Hz turbulence and the simulation results are shown in the following two figures.

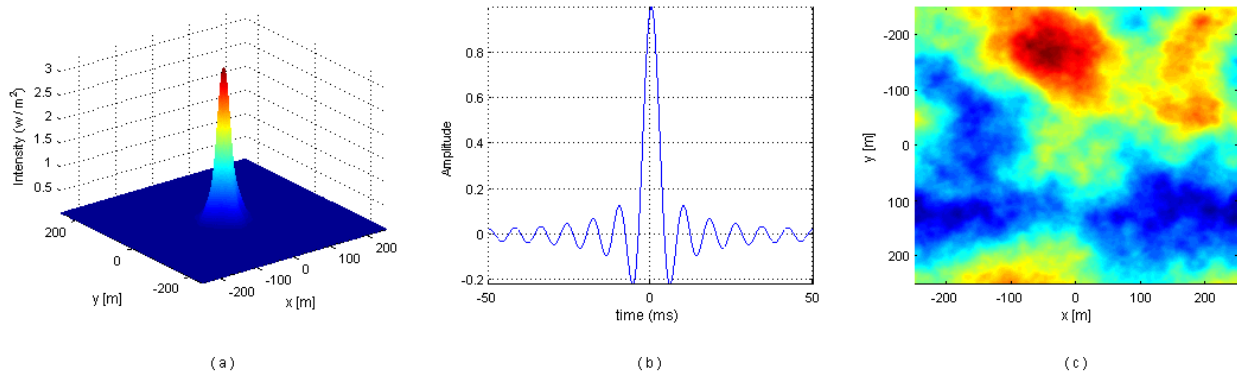


Fig.5. Propagation of EM waves through weak turbulence ($f_T = 50\text{Hz}$). (a) 3D Gaussian beam input ($w_0 = 30\text{mm}$); (b) modulating signal; and (c) random phase screen distribution profile.

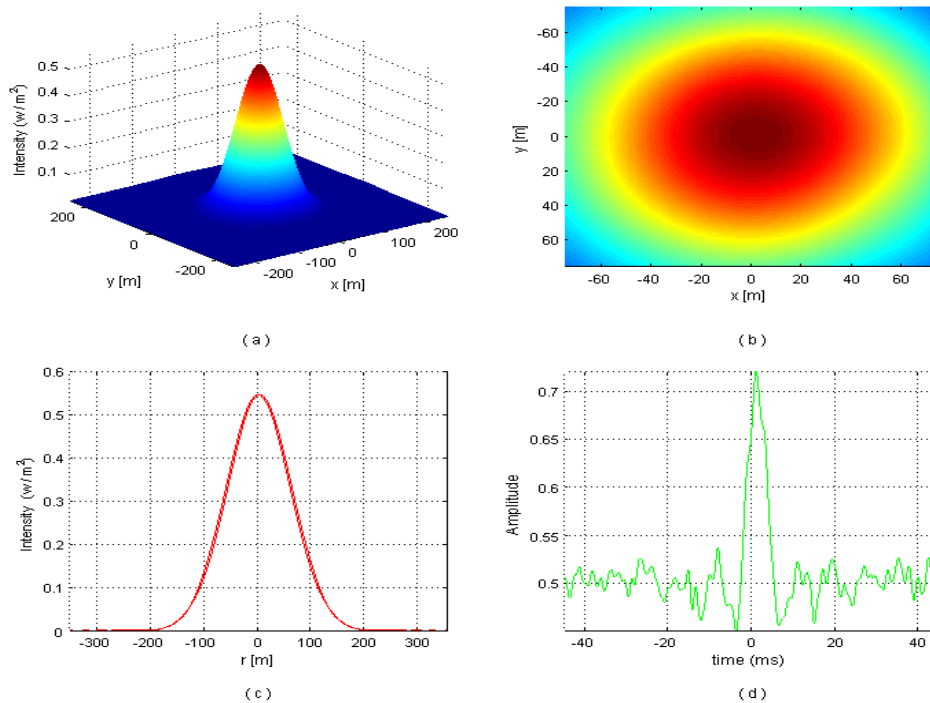


Fig.6. Propagation of EM waves through weak turbulence ($f_T = 50\text{Hz}$). (a) 3D Gaussian beam output ($w_0 \approx 80\text{mm}$); (b) cross-section of the output Gaussian intensity; (c) 2D output Gaussian profile; and (d) recovered signal.

We note from Figs. 5 and 6 that when the turbulence frequency increases, the received Gaussian profile begins to undergo some peak amplitude splitting (Fig.6(c)); additionally, the recovered superposed signal waveform shows even greater distortion (Fig.6 (d)).

c) Propagation through *weak* turbulence with mean frequency $f_T = 100\text{ Hz}$

Here we increase the turbulence frequency to 100 Hz. The numerical results are shown in Figs.7 and 8.

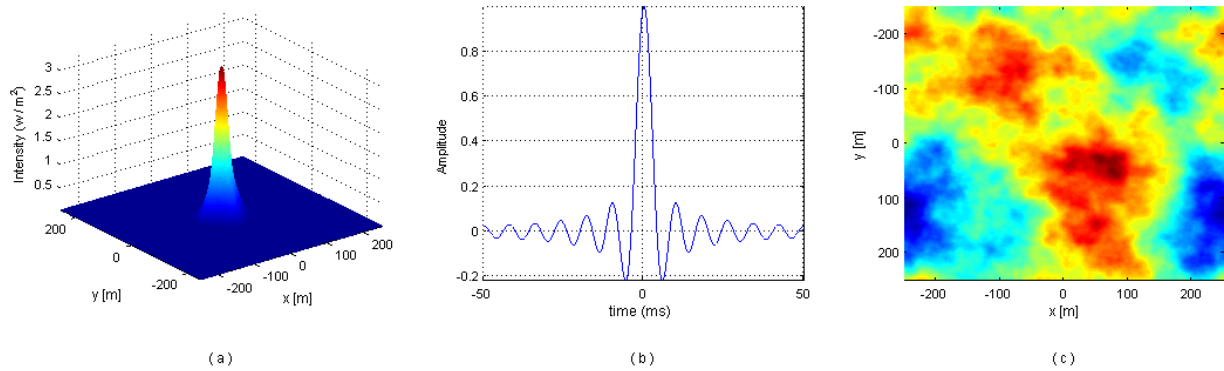


Fig.7. Propagation of EM waves through weak turbulence ($f_T = 100\text{Hz}$). (a) 3D Gaussian beam input ($w_0 = 30\text{mm}$); (b) modulating signal; and (c) random phase screen distribution profile.

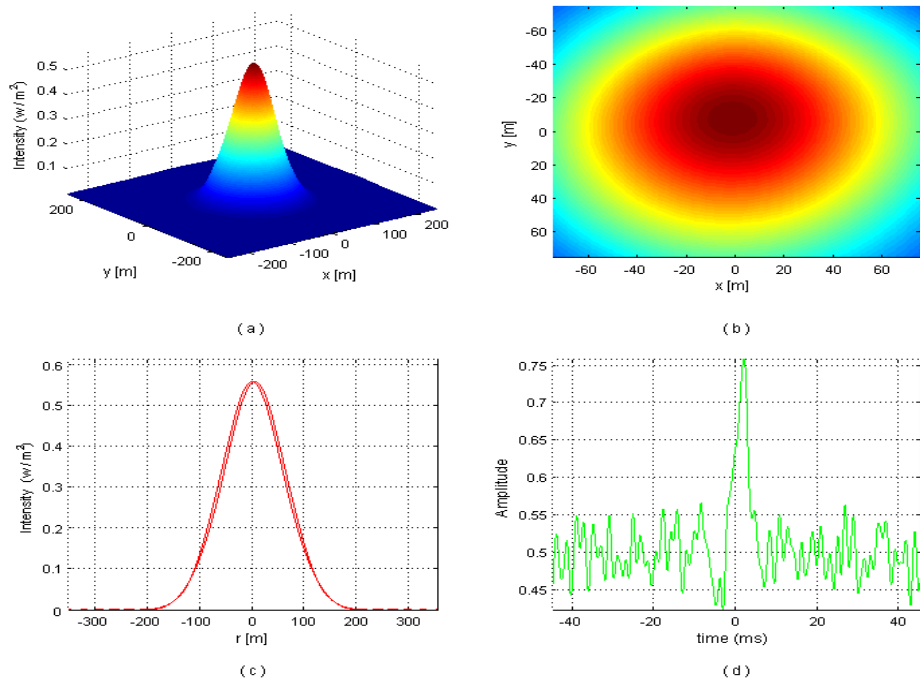


Fig.8. Propagation of EM waves through weak turbulence ($f_T = 100\text{Hz}$). (a) 3D Gaussian beam output ($w_0 \approx 80\text{mm}$); (b) cross-section of the output Gaussian intensity; (c) 2D output Gaussian profile; and (d) recovered signal.

Again, from the Figs.7 and 8, we observe that as the turbulence frequency increases, the Gaussian profile nominally broadened according to the Kirchhoff-Fresnel diffraction model begins to exhibit a small splitting in the transverse direction (Fig.8(c)). Moreover, the recovered signal likewise begins to get more distorted (Fig.8 (d)). This directly demonstrates the damaging effect of turbulence (with higher mean frequency) on a modulated EM wave even when the turbulence is relatively weak.

4.3 Propagation through *strong* turbulence

In this section, we examine the EM wave propagation for the case where the turbulence is made several orders of magnitude stronger. Accordingly, we choose $r_0 = 0.01 \text{ mm}$ with $C_n^2 = 1.067 \times 10^{-13} \text{ m}^{-2/3}$.

a) Propagation through *strong* turbulence with mean frequency $f_T = 20 \text{ Hz}$

In this case, we propagate the modulated EM waves along the propagation path with (mean) turbulence frequency 20 Hz and the simulation results are shown in Figs.9 and 10.

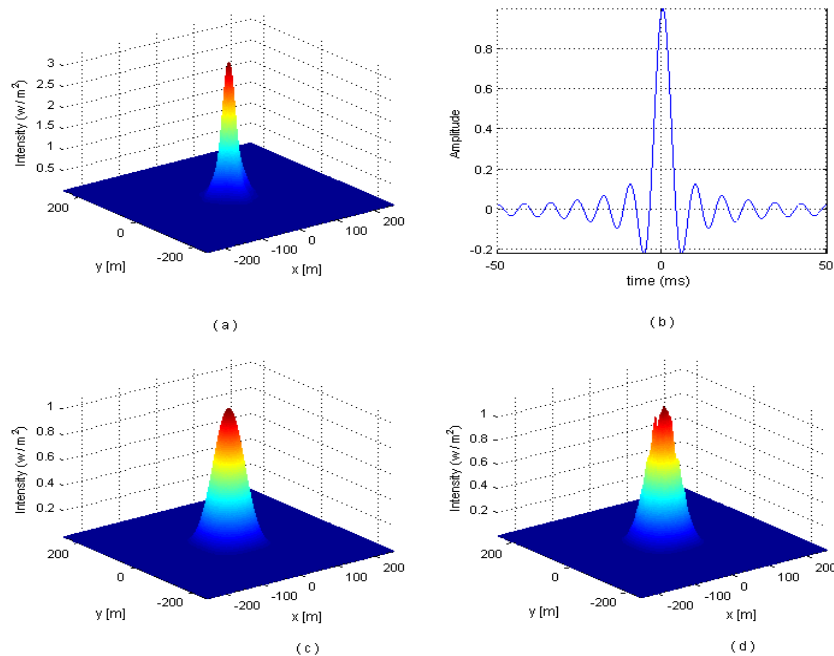


Fig.9. Propagation of EM waves through strong turbulence ($f_T = 20\text{Hz}$). (a) 3D Gaussian beam input ($w_0 = 30\text{mm}$); (b) modulating signal; (c) 3D field *before* the phase screen; and (d) 3D field *after* the phase screen.

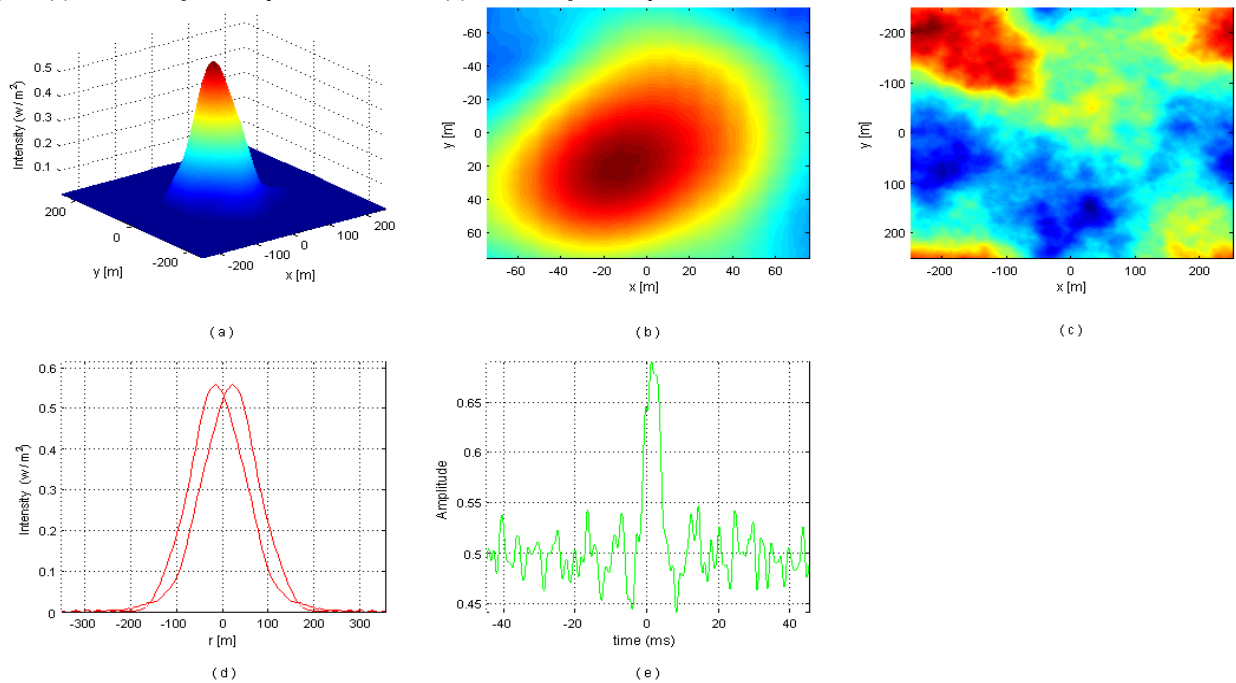


Fig.10. Propagation of EM waves through strong turbulence ($f_T = 20\text{Hz}$). (a) 3D Gaussian beam output ($w_0 \approx 80\text{mm}$); (b) cross-section of the output Gaussian intensity; (c) random phase screen distribution profile; (d) 2D output Gaussian profile; and (e) recovered signal.

From Fig.9, we now notice the impact of the random phase screen (representing strong turbulence) on the field profile *before* and *after* traversal across the screen. As seen in Fig.9 (d), the profile has undergone some amplitude distortion around the peak. In Fig.10, the EM profile undergoes even more radial splitting (Fig. (10d)). Another interesting feature to be noted is that following traversal through turbulence (whereby a peak distortion had occurred), the subsequent

diffraction broadening has likely “smoothened” out the peak distortion features immediately following the turbulence region (see Fig.10(a)). Also, the recovered signal suffers even greater amplitude distortion compared with the weak turbulence under the same turbulence frequency, as illustrated in Fig.10 (e).

b) Propagation through *strong* turbulence with mean frequency $f_T = 50$ Hz
 In the next series of simulation results, the mean turbulence frequency is increased to 50 Hz. The simulation results are shown in Figs.11 and 12.

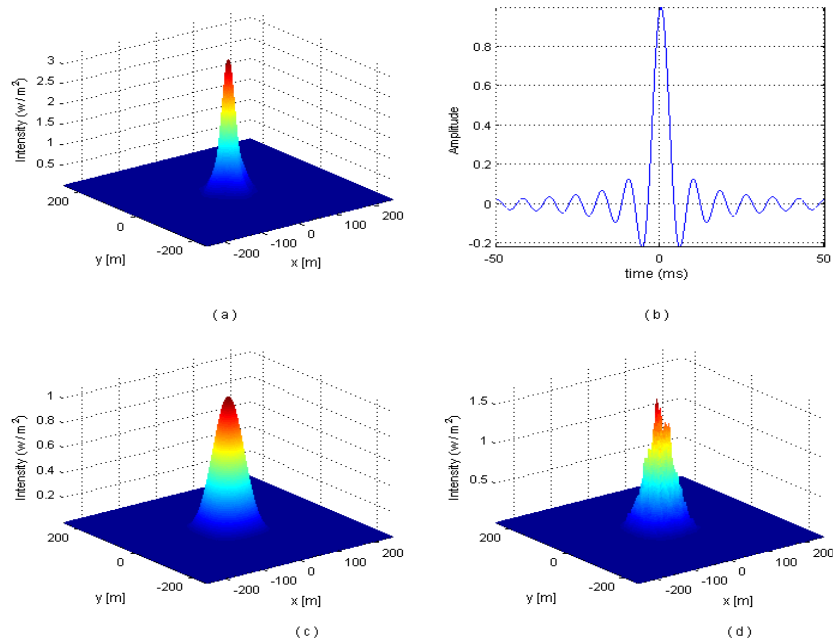


Fig.11. Propagation of EM waves through strong turbulence ($f_T = 50$ Hz). (a) 3D Gaussian beam input ($w_0 = 30$ mm); (b) modulating signal; (c) 3D field *before* the phase screen; and (d) 3D field *after* the phase screen.

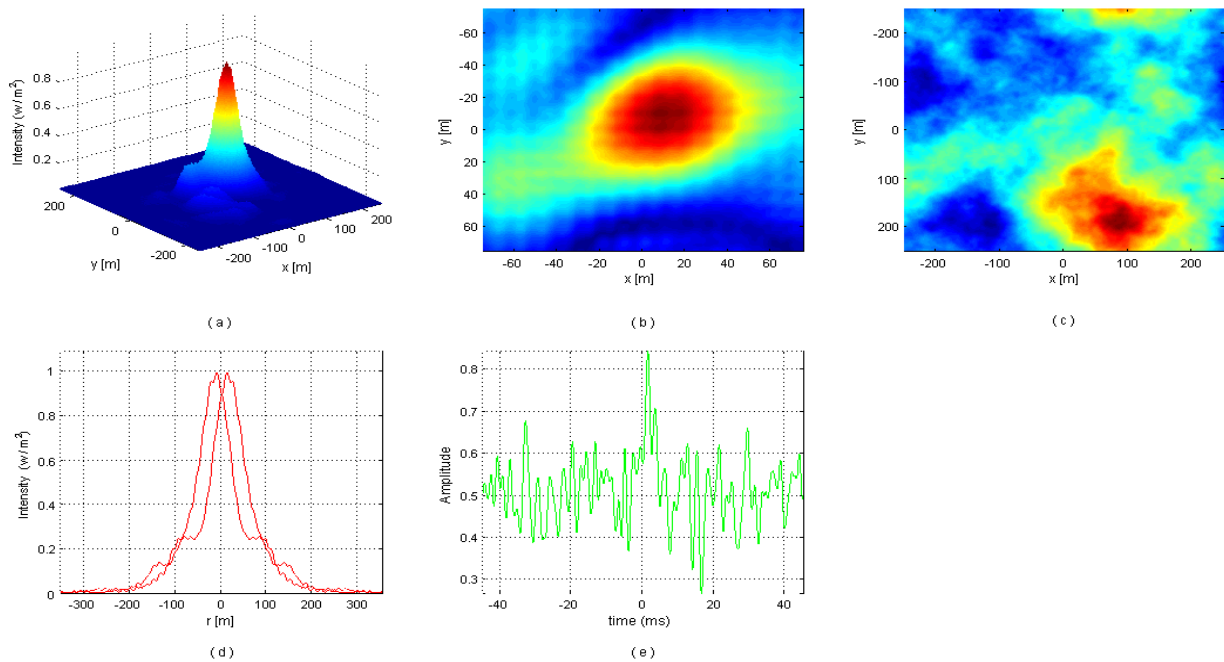


Fig.12. Propagation of EM waves through strong turbulence ($f_T = 50$ Hz). (a) 3D Gaussian beam output ($w_0 \approx 80$ mm); (b) cross-section of the output Gaussian intensity; (c) random phase screen distribution profile; (d) 2D output Gaussian profile; and (e) recovered signal.

The profile of the Gaussian beam gets more distorted now following the phase screen compared with the profile before the screen in a manner similar to the 20 Hz case (Figs.11(c) and (d)). In addition, we observe that the received Gaussian once again exhibits smoothing near the peak area; however, there occurs some additional distortion in the radially outward portion of the waveform (Fig.12 (a)). Also, the recovered signal distortion and Gaussian profile splitting scenarios indicate progressively greater magnitude when the mean turbulence frequency increases, as shown in Figs.12 (d) and (e).

c) Propagation through *strong* turbulence with mean frequency $f_T = 100$ Hz

Here we examine the effect of the propagation of modulated EM wave through strong turbulence with mean frequency 100Hz.

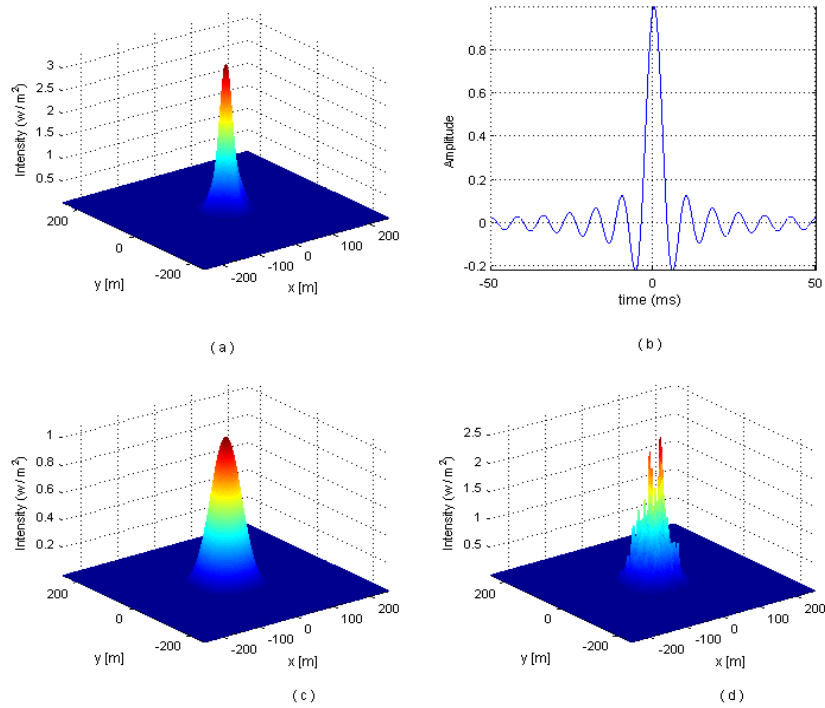


Fig.13. Propagation of EM waves through strong turbulence ($f_T = 100$ Hz). (a)3D Gaussian beam input ($w_0 = 30$ mm); (b) modulating signal; (c) 3D field *before* the phase screen; and (d) 3D field *after* the phase screen.

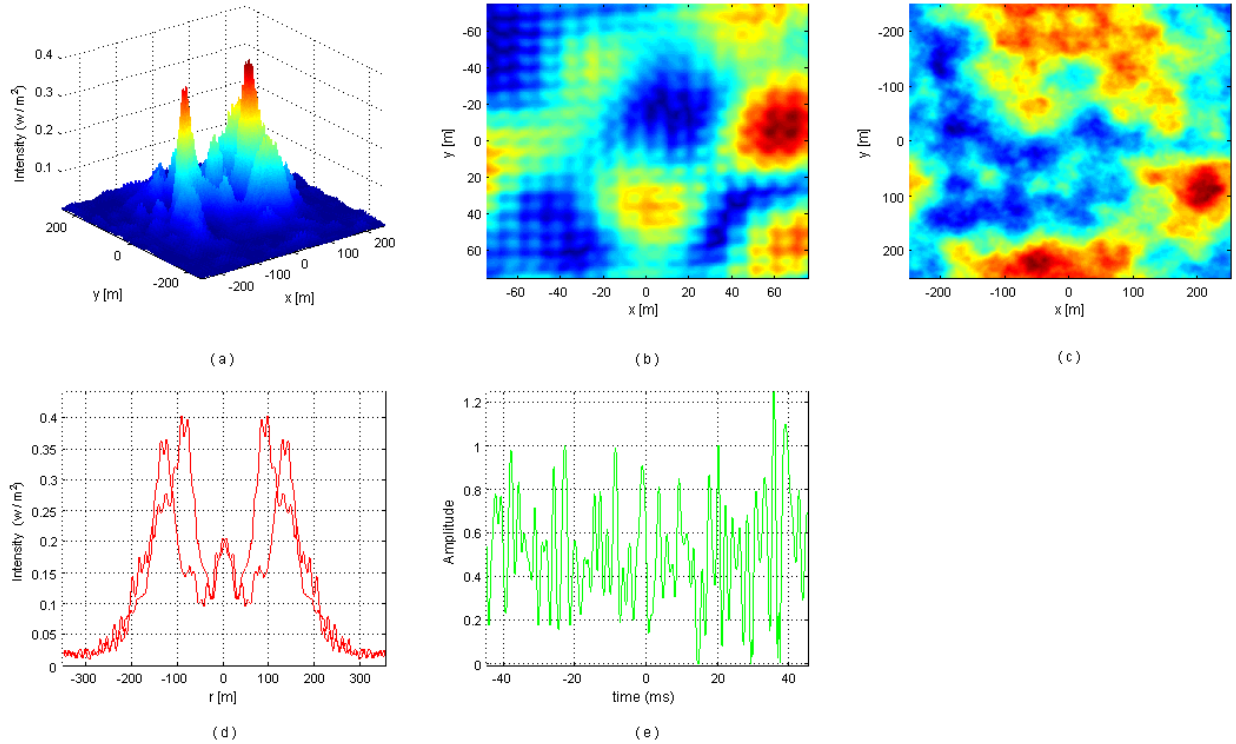


Fig.14. Propagation of EM waves through strong turbulence ($f_T = 100\text{Hz}$). (a) 3D Gaussian beam output; (b) cross-section of the output Gaussian intensity; (c) random phase screen distribution profile; (d) 2D output Gaussian profile; and (e) recovered signal.

The significance of the damaging effects of strong phase turbulence on the propagating Gaussian beam is self-evident from Figs.13 and 14. Thus, there is even greater peak distortion following passage across the phase screen (Fig.13(d)); similarly the received Gaussian beam now is split into spatially separated humps with peak smoothing and radial distortion (Fig.14(a) and (d)); finally, the sinc-signal waveform is distorted almost beyond recognition and is essentially pure amplitude noise (Fig.14(e)).

5. SPECTRAL APPROACH TO ENCRYPTED CHAOTIC WAVE PROPAGATION THROUGH TURBULENCE USING SVEA AND FOURIER TRANSFORMS

In this section, we intend to propagate a modulated chaotic wave through atmospheric turbulence. The AM modulation using chaos frequency may be expressed as [16,17]:

$$S_{ch}(t) = A_c [1 + ms(t)] \cos \omega_{ch} t \quad , \quad (14)$$

where m is the modulation index, and ω_{ch} is an equivalent chaos frequency. It has been verified that in an acousto-optic Bragg cell with first-order feedback, the time-dependent chaos wave generated is approximately amplitude modulated when the signal wave is applied via the RF (sound) input [16].

We note that the chaotic waveform in eq. (14) is essentially RF in nature, and manifests itself in the feedback loop as a current in the photodetector [16]. However, the chaos wave in turn rides on the optical carrier at the output of the Bragg cell (here assumed to be in first order), and is therefore manifested as *envelope modulation* of the optical carrier.

The modulated optical wave at the output of the Bragg cell may therefore be approximately written as (assuming AM/envelope modulation):

$$E_{AM}(x, y, z, t) = E_o(x, y, z) [1 + \tilde{m} S_{ch}(t)] \cos(\omega_o t - kz) \quad , \quad (15)$$

where \tilde{m} is the optical modulation index, ω_o is the optical frequency, $E_o(x, y, z)$ is the spatial profile of the optical wave as discussed earlier, and k in the unbounded wavenumber in the medium of propagation.

By substituting eqs.9 and 14 in 15, we get (assuming Gaussian optical profile):

$$E_{AM}(x, y, z, t) = A \frac{w_0}{w(z)} e^{-\frac{(x^2+y^2)}{w^2(z)}} \{1 + A_c \tilde{m} [1 + ms(t)] \cos \omega_{ch} t\} \cos(\omega_0 t - kz). \quad (16)$$

As mentioned, we have here two levels of AM modulation. We will follow the same process by propagating the chaos-modulated optical carrier along the propagation distance from the transmitter to the receiver, and include the random phase screen located mid-way when incorporating turbulence. Also, we will use SVEA approximation because the optical carrier is orders of magnitude faster than either the chaotic or the signal waveforms. As described, a sinc-type message waveform is therefore embedded onto the chaotic carrier at the output of a Bragg cell (not shown here; see ref. [16] for details). The resulting numerical data for the encrypted chaos wave is used to amplitude-modulate the optical carrier. It must be noted that for the case where information is used to directly modulate the optical carrier (as described in section 3), photo detection automatically transfers the intensity corresponding to the envelope, and the optical carrier is eliminated. Thereafter, signal recovery involves simple electronic processing. For the case of a *chaotic* envelope riding the optical carrier, however, photo detection will at first result in a scaled version of the modulated chaos to be detected via the photocurrent. Eventually, the heterodyne receiver strategy with appropriate cut-off frequency may be used to retrieve the baseband (message) signal.

6. NUMERICAL SIMULATIONS, RESULTS AND INTERPRETATIONS

6.1 A uniform (non-turbulent) propagation prototype

In this case, we examine the propagation of chaotic EM waves through a uniform medium. Normally, transmission and recovery of time-modulated EM wave through uniform or homogeneous media is fairly standard and well-established, and does not require any examination as such. However, the purpose of including this propagation problem prior to introducing turbulence is three-fold. First, the time-modulated signal is being propagated over a homogenous region wherein we incorporate the diffractive effects along the path. Since diffraction is essentially a spatial phenomenon, our interest is to ascertain the effect of spatial diffraction on the time signal carried within the modulated chaotic carrier. Second, we wish to determine whether standard demodulation strategies will enable extraction of the message from the photo-detector response at the receiver. Third, the recovery in this case relates to a message carried within a chaotic wave; retrieval of the message therefore needs special consideration vis-à-vis the properties of the chaos wave as opposed to a standard sinusoidal carrier. The simulation results are shown in the following two figures.

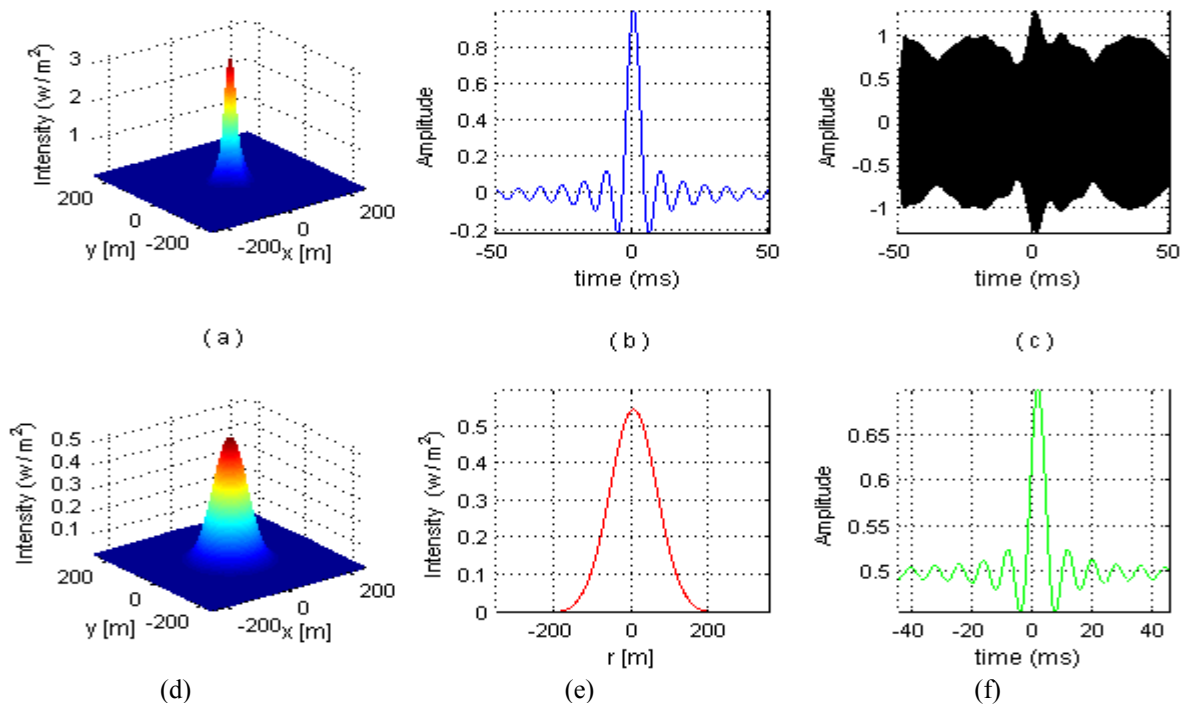


Fig. 15. Propagation of modulated chaotic waves through a uniform medium. (a) 3D Gaussian beam input ($w_0=30mm$); (b) modulating signal; (c) modulated signal; (d) 3D Gaussian beam output; (e) 2D output Gaussian profile; and (f) recovered signal.

From Fig.15, we observe that the profile of the EM beam is broadened due to diffraction during passage through the (homogenous) medium (Fig.15 (a) and (d)). Also, Fig.15 (f) shows that the received signal is recovered without any distortion using a simple heterodyne receiver used to filter out the chaos frequency and its harmonics in the photocurrent, thereby enabling recovery of the message signal [16].

6.2 Chaotic propagation through *weak* turbulence with mean frequency $f_T = 50$ Hz

Here, we propagate the chaotic EM wave through narrow and weak turbulence with mean frequency of 50Hz. For weak turbulence, we choose $r_0 = 10$ mm with $C_n^2 = 1.067 \times 10^{-18} \text{ m}^{-2/3}$; the corresponding simulation results are illustrated in Fig.16.

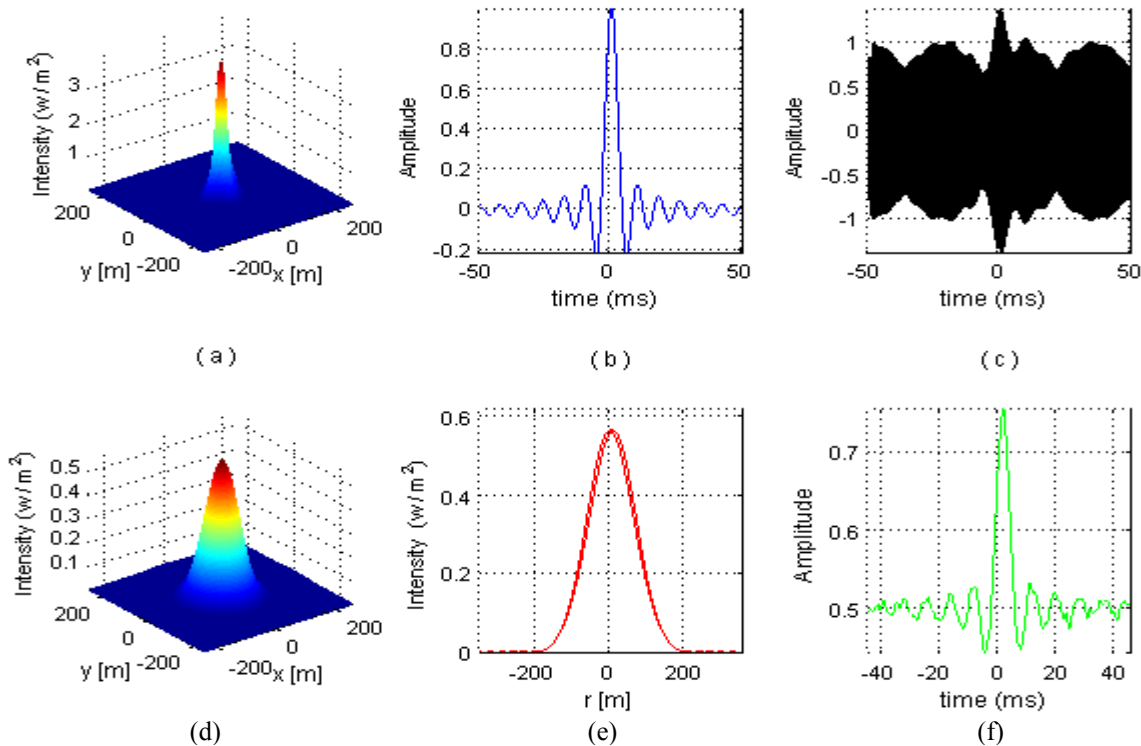


Fig.16. Propagation of modulated chaotic waves through weak turbulence ($f_T = 50$ Hz). (a) 3D Gaussian beam input ($w_0 = 30$ mm); (b) modulating signal; (c) modulated signal; (d) 3D Gaussian beam output; (e) 2D output Gaussian profile; and (f) recovered signal.

In the presence of turbulence (here weak), we find that the diffracted beam profile (Fig.16 (d) and (e)) begins to exhibit radial splitting (rather small for the weak case; see Fig.16 (e)). As may be recalled, even under weak turbulence, transmission of a directly modulated EM wave results in significant distortion of the recovered signal (see Fig.6 (d)). When the message is embedded in a chaotic carrier, it is seen that even after passage through relatively weak chaos, the message is recovered with noticeably higher integrity (see Fig.16 (f)). Although this finding is relatively limited in scope, it nevertheless holds out the promise that a message wave may be secured and protected from a turbulent environment by packaging it inside a chaos wave via the RF encryption methodology which has been developed by our group [16,17]. As is shown later, when the turbulence becomes stronger, the recovery of the message from the chaos wave is subject to some degree of distortion, and is not entirely distortion-free. However, the results indicate that packaging a message in a chaos wave does still offer some immunity from even stronger turbulence compared with non-chaotic transmission.

6.3 Chaotic propagation through *strong* turbulence with mean frequency $f_T = 50$ Hz

In the case of strong turbulence, we choose $r_0 = 0.01$ mm with $C_n^2 = 1.067 \times 10^{-13} \text{ m}^{-2/3}$.

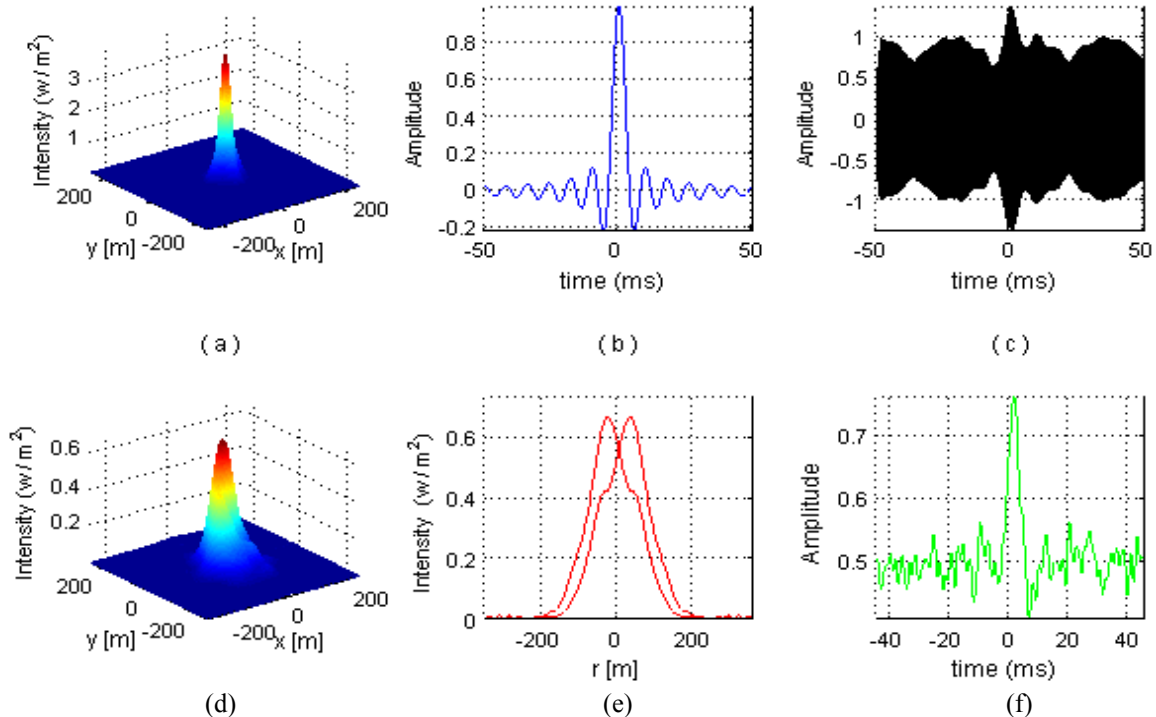


Fig.17. Propagation of modulated chaotic waves through strong turbulence ($f_T = 50$ Hz). (a) 3D Gaussian beam input ($w_0 = 30$ mm); (b) modulating signal; (c) modulated signal; (d) 3D Gaussian beam output; (e) 2D output Gaussian profile; and (f) recovered signal.

Fig.17 shows the simulation results for propagation of the modulated chaotic wave over a medium under strong turbulence. It is evident that under strong turbulence, the diffracted profile is even further split in the radial direction (see Fig.17 (e)). For this case, the signal recovered using the heterodyne strategy is noticeably distorted (Fig.17 (f)); however, the degree of distortion is considerably lower than that obtained for non-chaotic propagation (see Fig.12 (e) for comparison). The above further reinforces the observation that chaotic encryption likely immunizes a message waveform from the damaging effects of turbulence.

7. CONCLUDING REMARKS

In this paper, an alternative approach was used to examine the propagation of non-chaotic and chaotic waves through both non-turbulent media and phase-turbulent atmosphere. The propagation of an optical carrier (with a non-chaotic or chaotic envelope) was investigated using the SVEA approximation. The propagation process including the use of (spatial) Fourier transforms and the Kirchhoff-Fresnel integral were carried out on the basis of complex phasors representing the scalar fields. The propagation of the modulated EM wave through random phase turbulence was examined under different atmospheric conditions, viz., uniform (non-turbulent) and turbulent (weak or strong), the latter under different time fluctuations of the turbulence. In the case of direct modulation of the EM carrier (without chaotic envelope), the received signal following photodetection was obtained using standard electronics. When encrypted chaos was incorporated into the optical carrier, a heterodyne receiver strategy with appropriate cut-off frequency was used to extract the received (message) signal from the chaotic carrier in the photocurrent. For propagation in a uniform atmosphere, results indicated received signals which were scaled versions of the transmitted signal under direct, non-chaotic modulation. When turbulence was introduced, and its average temporal frequency was increased (assuming 20, 50 and 100 Hz), the EM output beam began to experience radial splitting, and the recovered signal became increasingly

distorted. Moreover, the simulations showed that the recovered signal underwent greater distortion when the turbulence was made stronger. Thus, non-chaotic signals riding an optical carrier suffered greater distortion under both turbulence of higher average temporal frequency. More significantly, when chaos was introduced as an encrypted carrier, it was found that the recovered signal suffered considerably less distortion under similar turbulence and medium conditions. These results indicate that embedding a message signal inside a chaos wave prior to transmission via an EM wave over a (phase) turbulent medium may reduce the degree of signal distortion which otherwise occurs under non-chaotic transmission. Further examination of this phenomenon is currently under study.

REFERENCES

- [1] X. Zhu and J.M. Kahn, "Free-space optical communication through atmospheric turbulence channels," *IEEE Trans. Comm.* 50(08), 12931300 (2002).
- [2] V.S. Rao Gudimetlaa, R.B. Holmesb, T.C. Farrella, and J. Lucas, "Phase screen simulations of laser propagation through non-Kolmogorov atmospheric turbulence," *Proc. SPIE* 8038, 803808-1-12 (2011).
- [3] L. C. Andrews, R. L. Phillips and A. R. Weeks, "Propagation of a Gaussian-beam wave through a random phase screen," *Waves in Random Media (UK)*, 7, 229-244 (1997).
- [4] V.I. Tatarski, A. Ishimaru, V.U. Zavorotny, [Wave Propagation in Random Media (Scintillation)], SPIE Press, Seattle, Washington(1992).
- [5] M.R. Chatterjee and F.H.A. Mohamed, "A Transfer Function Based Frequency Model for Propagation of a Chaos Wave through Modified von Karman Turbulence under Various Chaos and Turbulence Conditions", OSA Topical Meeting on Imaging and Applied Optics, Arlington, VA, (2015).
- [6] M.R. Chatterjee and F.H.A. Mohamed, "Spectral and Performance Analysis for the Modified von Karman Turbulence", OSA Annual Meeting (FiO/LS), San Jose, CA, (2015).
- [7] G. P. Agrawal, [Nonlinear Fiber Optics], 5th ed., Academic Press, NY, Oct. (2012).
- [8] N. J. Miller, P. F. Widiker, P. F. McManamon, and J.W. Haus, "Active multi-aperture imaging through turbulence," *Proc. SPIE*, vol. 8395, pp. 839504-1-10, May (2012).
- [9] J. W. Goodman, [Introduction to Fourier Optics], 2nd ed., McGraw-Hill, NY, (1996).
- [10] K. Iizuka, [Engineering Optics], 3rd ed., Springer-Verlag, Berlin, May (2009).
- [11] J. D. Schmidt, [Numerical Simulation of Optical Wave Propagation with Examples in Matlab], SPIE, Bellingham, WA, (2010).
- [12] D. Voelz, [Computational Fourier Optics (A MATLAB Tutorial)], SPIE Press, Bellingham, WA, (2011).
- [13] A. Papoulis, [Probability, Random Variables, and Stochastic Processes], McGraw-Hill, Inc., USA (1965).
- [14] P.P. Banerjee and T. Poon, [Principles of Applied Optic], Richard D. Irwin, Inc., and Aksen Associates, Inc., USA, (1991).
- [15] J.M. Jarem, [Computational Methods for Electromagnetic and Optical Systems], 2nd ed., NY, (2011).
- [16] M. R. Chatterjee, M. Alsaedi, "Examination of chaotic signal encryption and recovery for Secure communication using hybrid acousto-optic feedback," *Opt. Eng.* 50(5), 055002-1-14, (2011).
- [17] M. R. Chatterjee, F. S. Almeahmadi, "Numerical examination of acousto-optic Bragg interactions for profiled light waves using a transfer function formalism", SPIE Photonics West, San Francisco, CA, Oct. (2013).